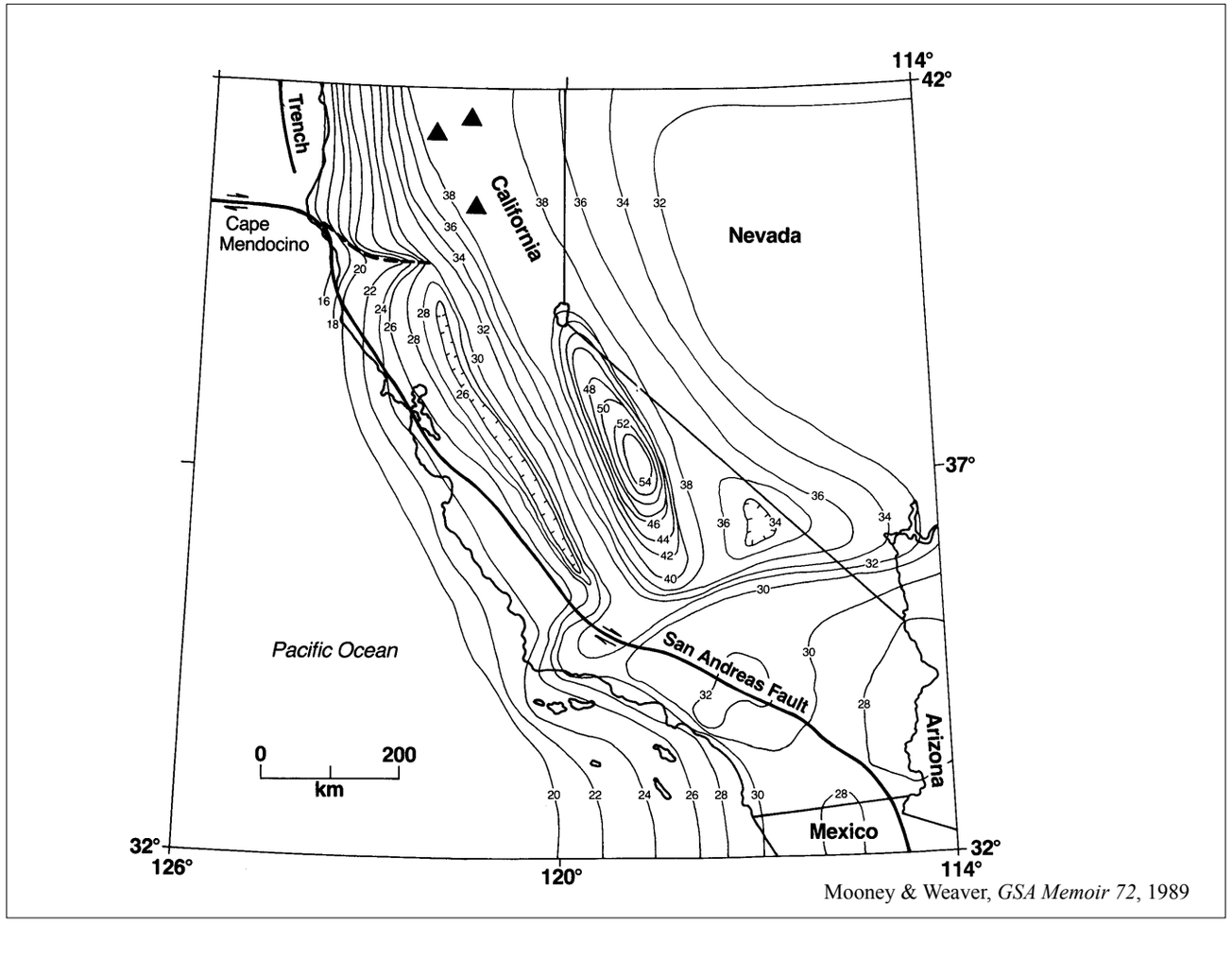

Mooney & Weaver, *GSA Memoir 72*, 1989

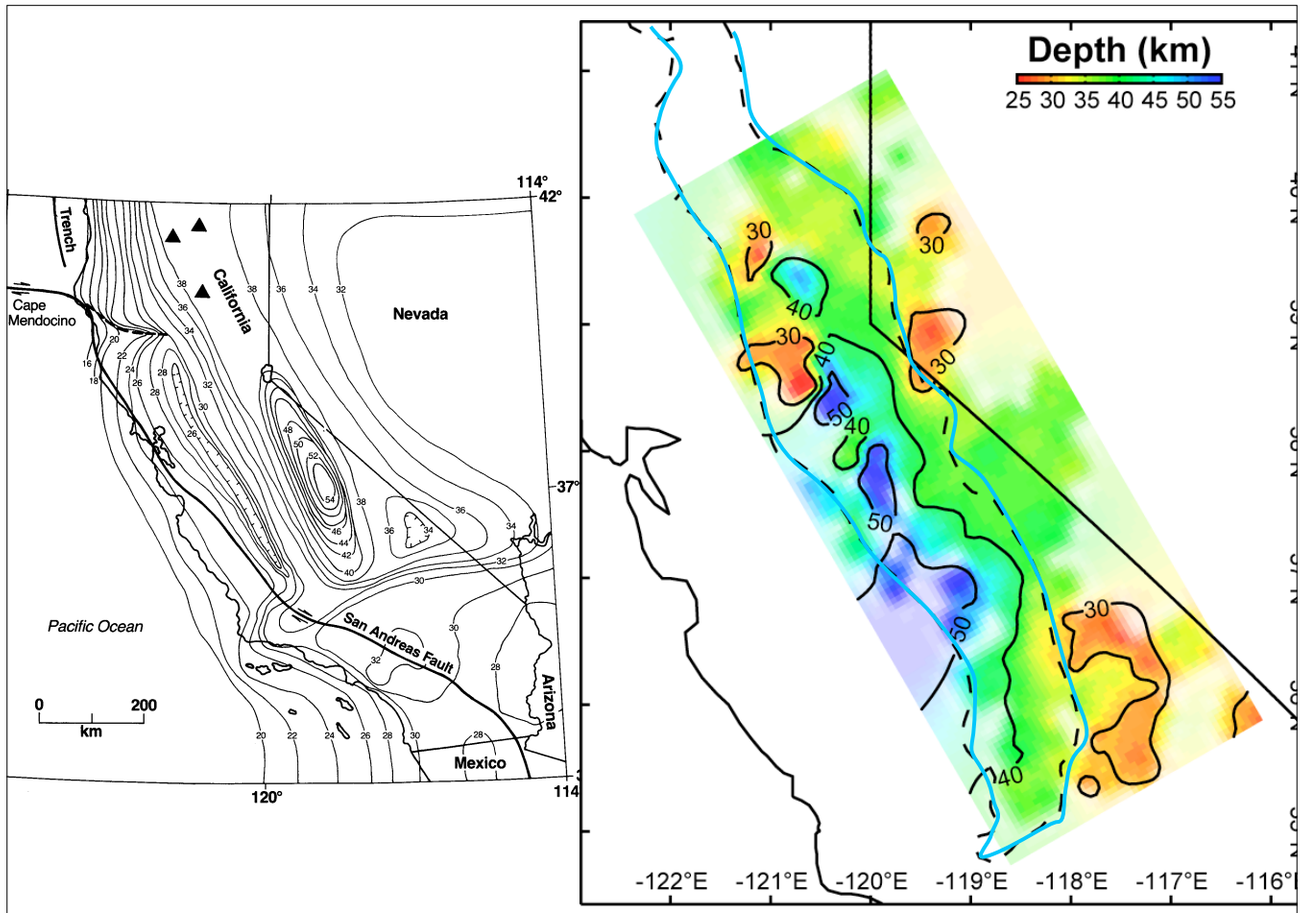

Mooney & Weaver, *GSA Memoir 72*, 1989

Frasetto et al., *Geosphere*, 2011

Big incompatibility here. What is the deal?

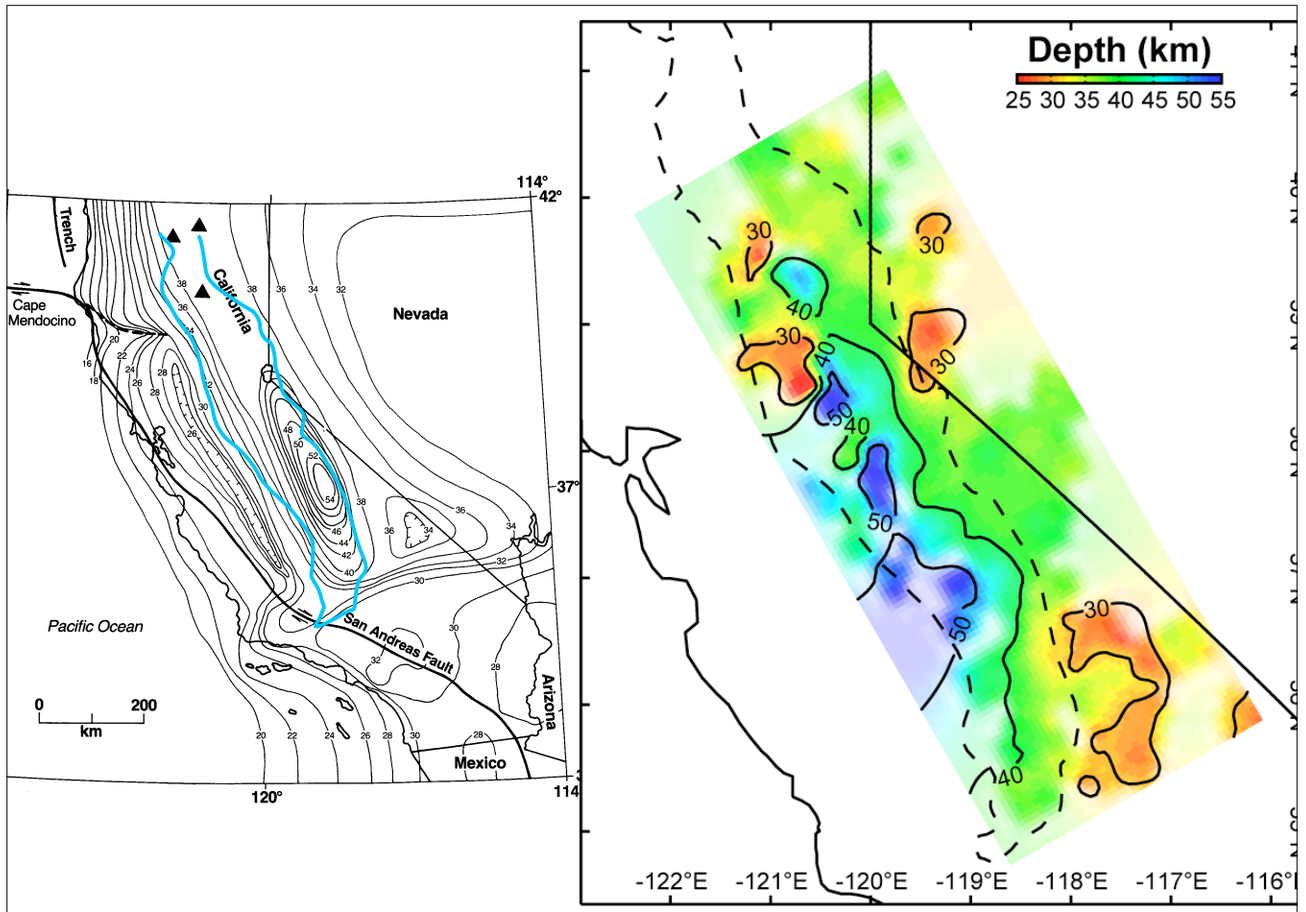

Mooney & Weaver, *GSA Memoir 72*, 1989

Frasetto et al., *Geosphere*, 2011

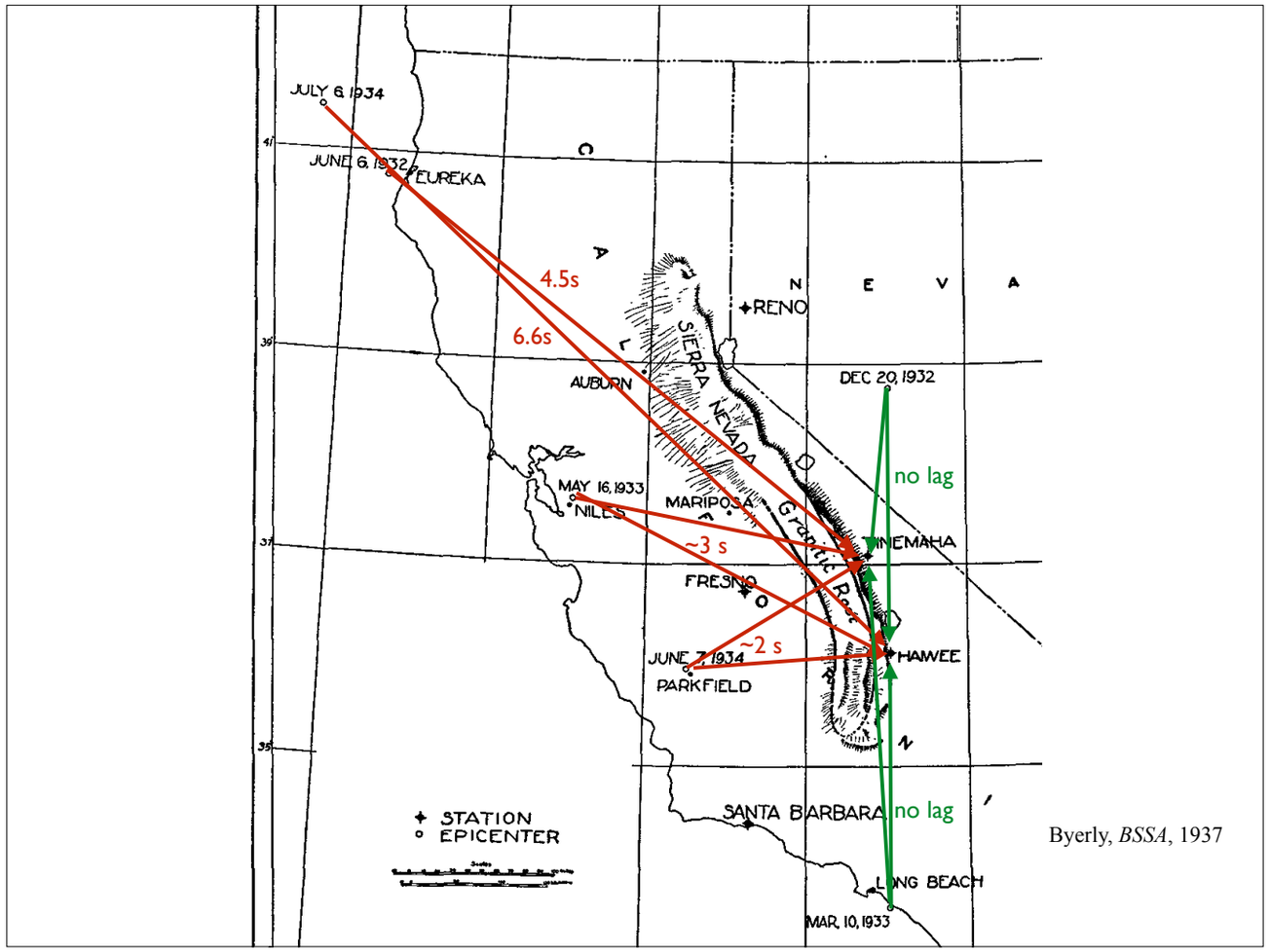

Byerly, *BSSA*, 1937

Times are delays from expected arrival time. No lag from EQs near Eureka to Fresno. Also no lag in Pg.

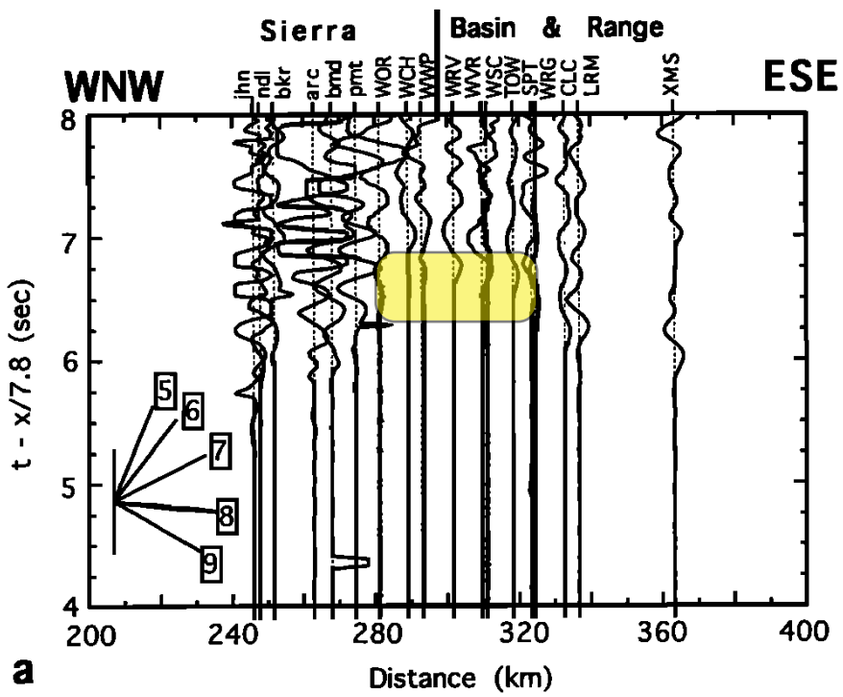

EQs on west of Sierra: Arrival late

Savage et al., *Tectonics*, 1994

Arrivals at station just east of the Sierra late for events from west--this section shows what that looks like.

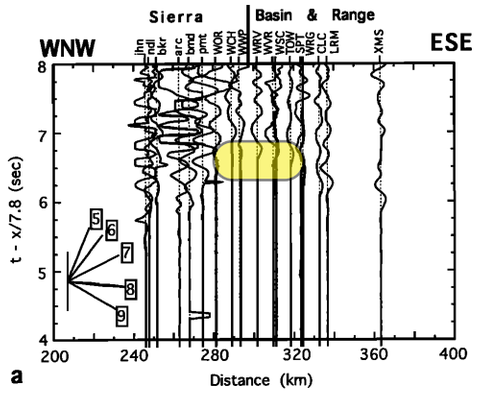

Byerly 1938

EQs on west of Sierra: Arrival late

Savage et al., *Tectonics*, 1994

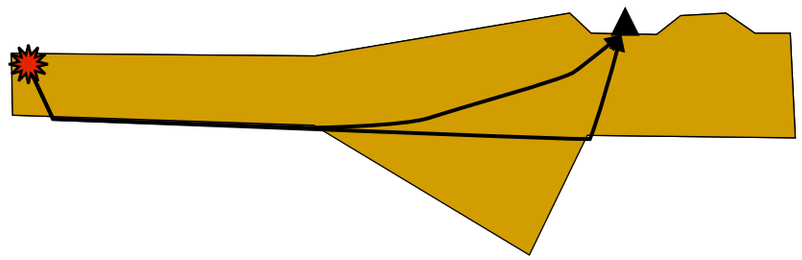

That was the seismic observations…was there support elsewhere?

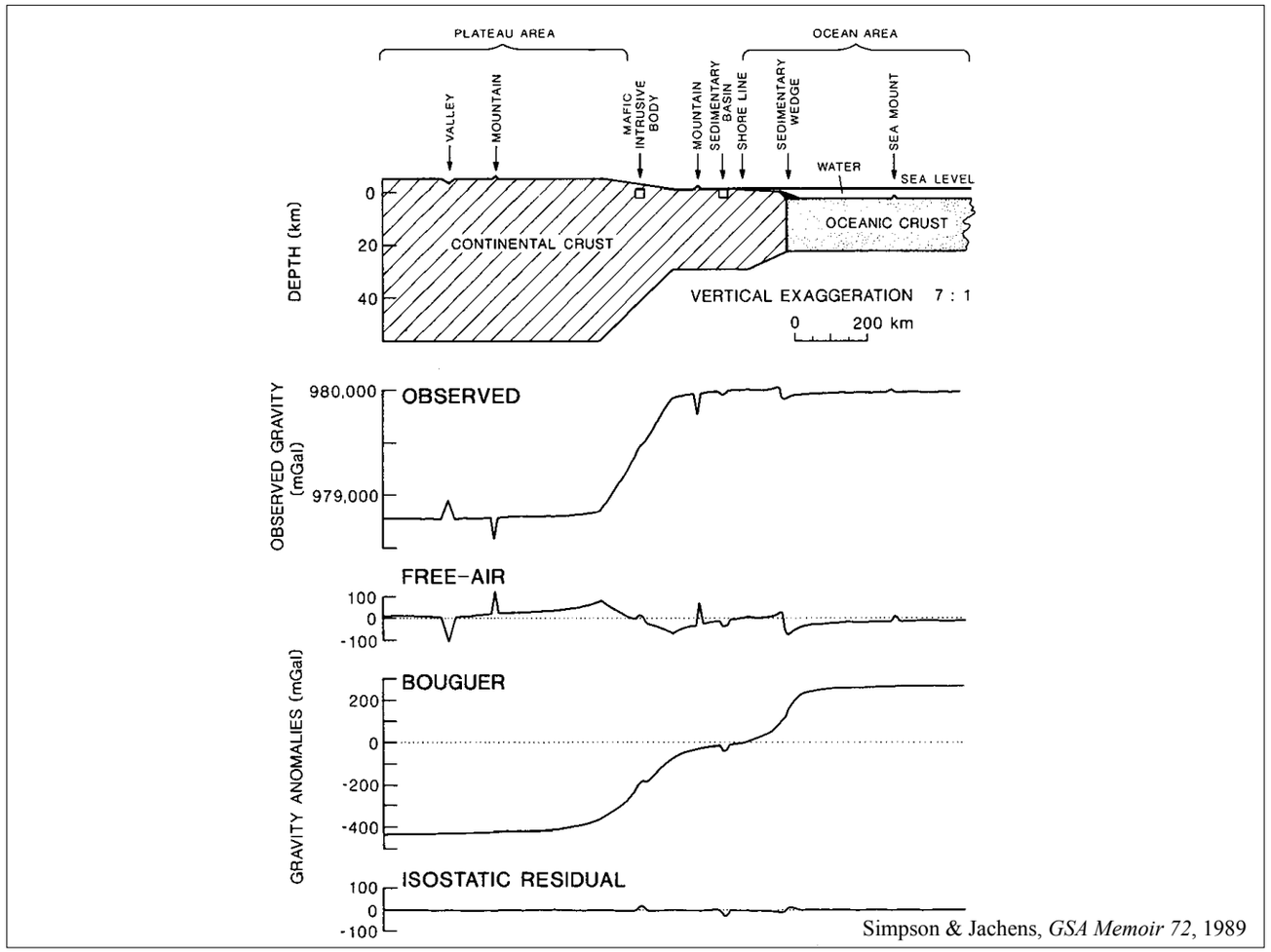

Simpson & Jachens, *GSA Memoir 72*, 1989

First we need to have a basic idea of how gravity anomalies work.

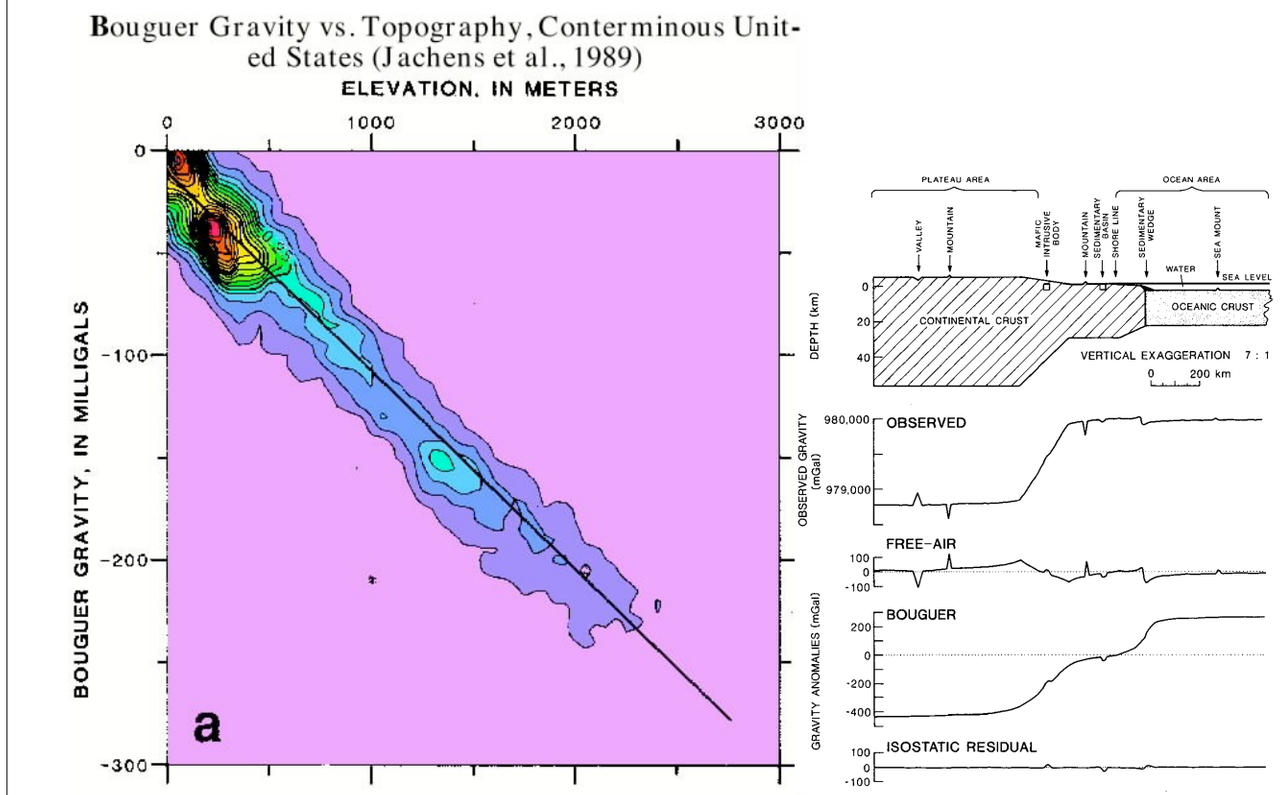

…in essence, we find that gravity anomalies are smaller (more negative) the higher you go, indicating isostasy is active.

Gravity Profile across Sierra

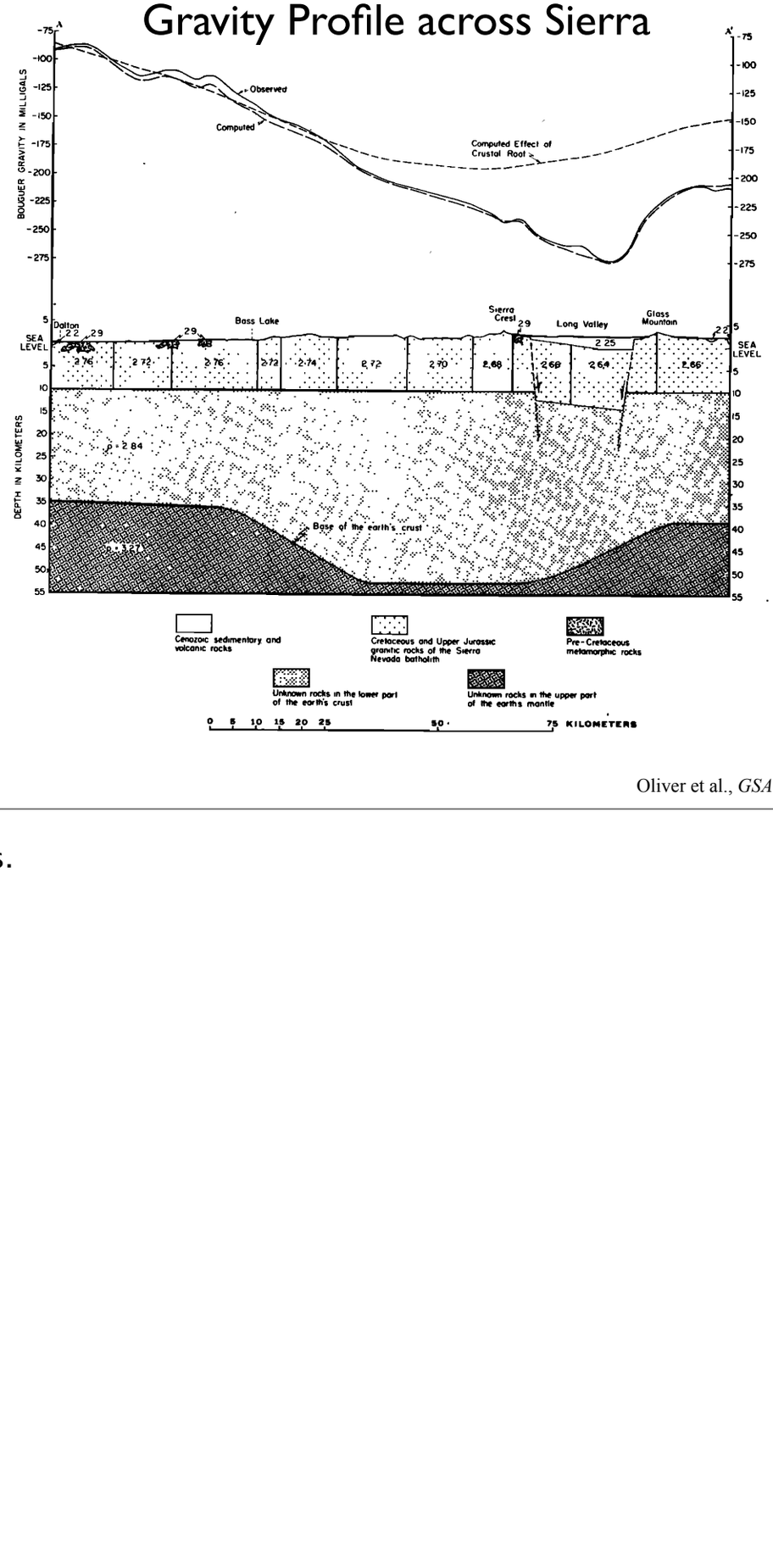

Oliver et al., *GSA Bull*, 1961

…but there are multiple ways of interpreting this.

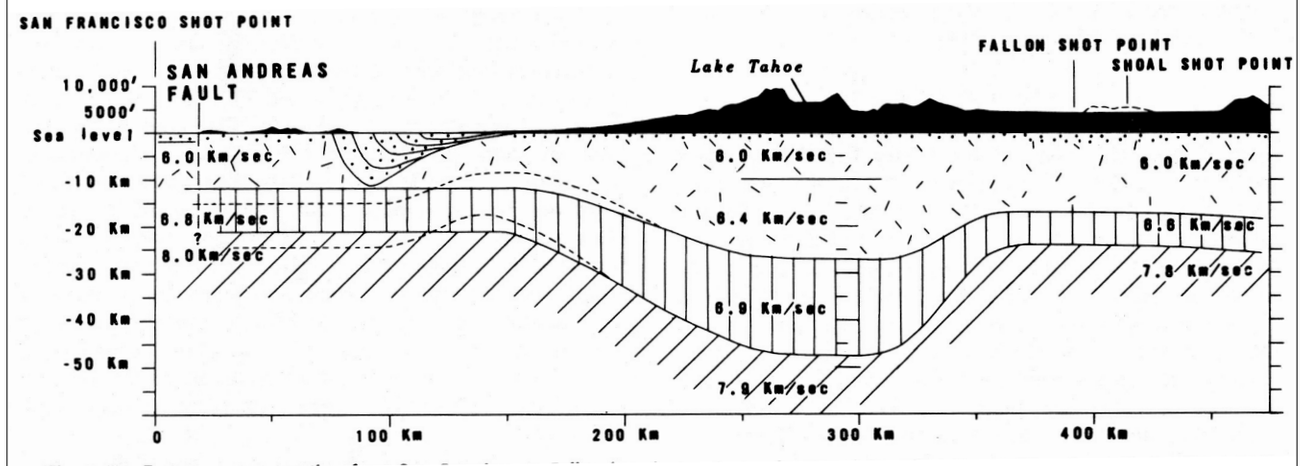

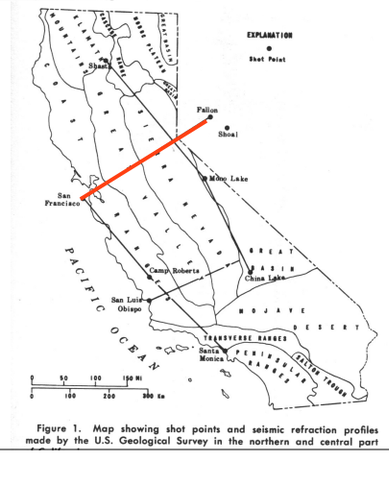

Figure 1. Map showing shot points and seismic refraction profiles made by the U.S. Geological Survey in the northern and central part

Eaton, *CDMG Bull 190*, 1966

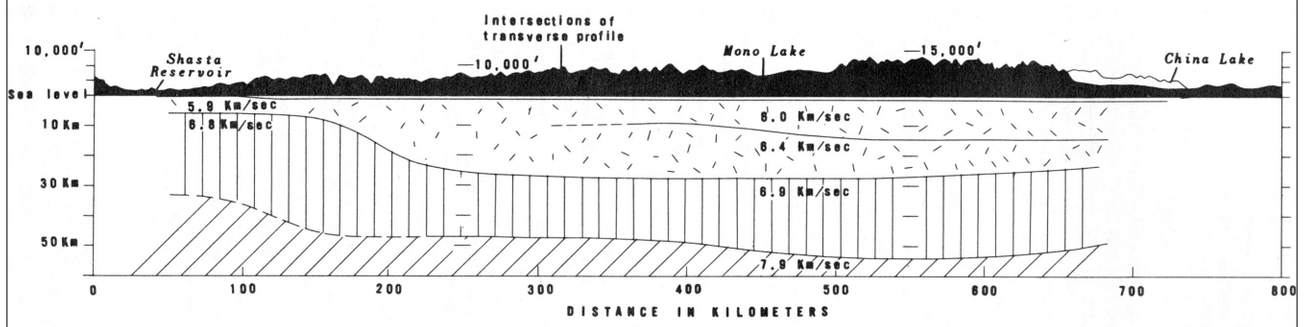

Figure 2. Longitudinal seismic cross section through the Sierra Nevada from near Shasta Reservoir to China Lake.

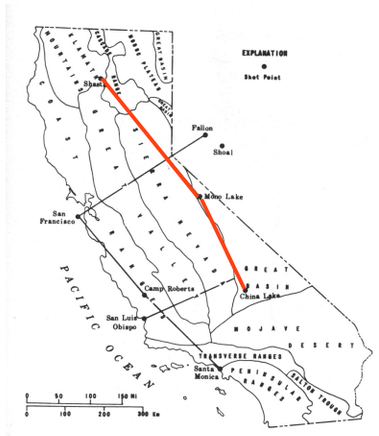

Figure 1. Map showing shot points and seismic refraction profiles made by the U.S. Geological Survey in the northern and central part

Table 1. Traveltime curves of the Sierra Nevada refraction profile.

Phase	*Traveltime line*	*Nature and range of arrival*
(Mono Lake to China Lake)		
P_g	$1.0 + \Delta/6.0$	First arrival, 10 to 135 km
P^*_1	$2.6 + \Delta/6.4$	First arrival, 135 to 205 km
P^*_2	$4.7 + \Delta/6.9$	Reflections primarily, 100 to 230 km
P_n	$10.6 + \Delta/8.1$	First arrival, 280 to 310 km, and reflections, 150 to 250 km
(China Lake to Mono Lake)		
P_g	$1.1 + \Delta/6.1$	First arrival, 5 to 160 km
P^*_1	$2.3 + \Delta/6.3$	Reflections, 55 to 170 km
P^*_2	$4.2 + \Delta/6.9$	First arrival beyond 160 km
P_n	$8.7 + \Delta/7.7$	Reflections, 100 to 250 km, and Mono Lake to China Lake reciprocal point

Eaton, *CDMG Bull 190*, 1966

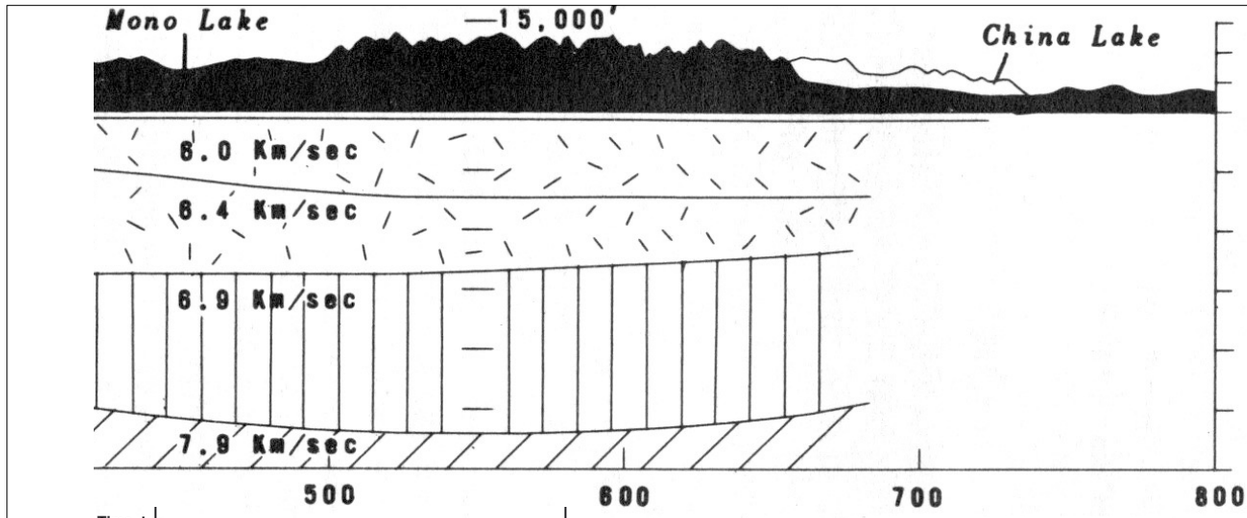

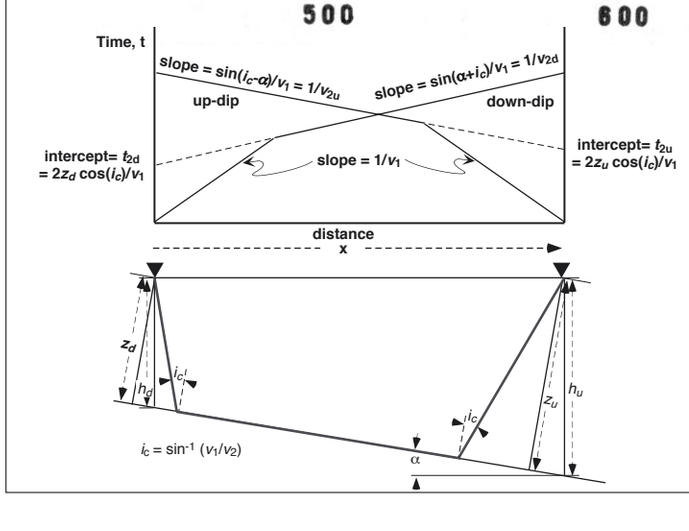

Table 1. Traveltime curves of the Sierra Nevada refraction profile.

Phase	*Traveltime line*	*Nature and range of arrival*
(Mono Lake to China Lake)		
P_g	$1.0 + \Delta/6.0$	First arrival, 10 to 135 km
P^*_1	$2.6 + \Delta/6.4$	First arrival, 135 to 205 km
P^*_2	$4.7 + \Delta/6.9$	Reflections primarily, 100 to 230 km
P_n	$10.6 + \Delta/8.1$	First arrival, 280 to 310 km, and reflections, 150 to 250 km
(China Lake to Mono Lake)		
P_g	$1.1 + \Delta/6.1$	First arrival, 5 to 160 km
P^*_1	$2.3 + \Delta/6.3$	Reflections, 55 to 170 km
P^*_2	$4.2 + \Delta/6.9$	First arrival beyond 160 km
P_n	$8.7 + \Delta/7.7$	Reflections, 100 to 250 km, and Mono Lake to China Lake reciprocal point

Eaton, *CDMG Bull 190*, 1966

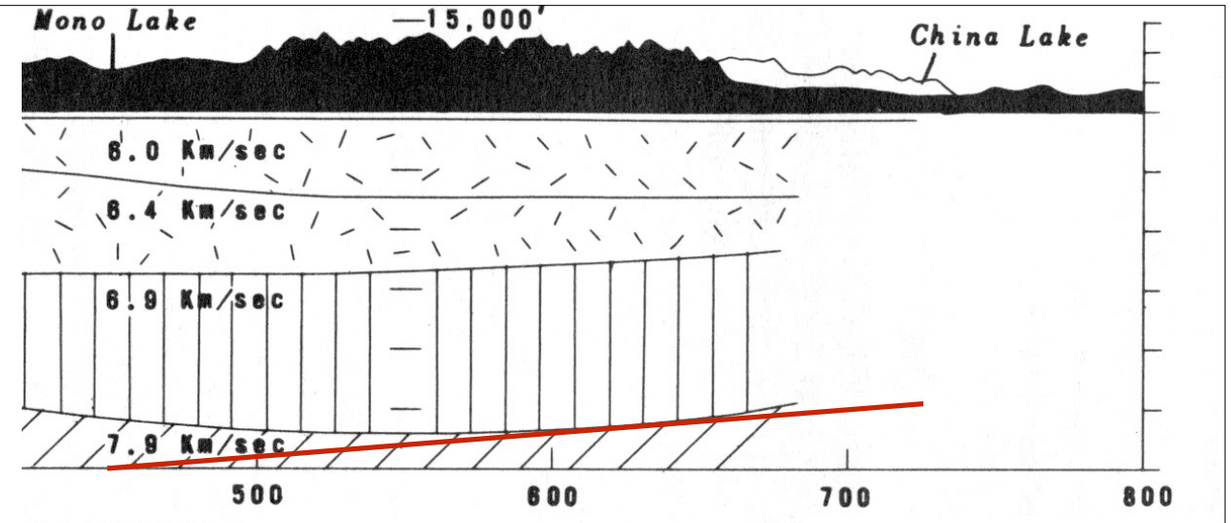

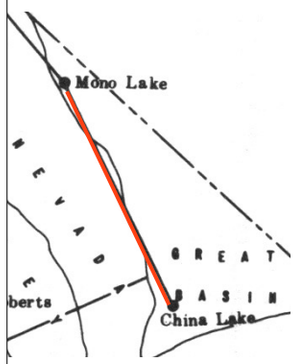

If we approximate crust as 6.55 km/s, then:
From intercepts:
Moho at Mono Lake end 60 km bsl
Moho at China Lake end 50 km bsl
Dip of 2.0°

From apparent velocities:
Dip to north of 2.2°
Velocity of 7.9 km/s

Table 1. Traveltime curves of the Sierra Nevada refraction profile.

Phase	*Traveltime line*	*Nature and range of arrival*
(Mono Lake to China Lake)		
P_g	$1.0 + \Delta/6.0$	First arrival, 10 to 135 km
P^*_1	$2.6 + \Delta/6.4$	First arrival, 135 to 205 km
P^*_2	$4.7 + \Delta/6.9$	Reflections primarily, 100 to 230 km
P_n	$10.6 + \Delta/8.1$	First arrival, 280 to 310 km, and reflections, 150 to 250 km
(China Lake to Mono Lake)		
P_g	$1.1 + \Delta/6.1$	First arrival, 5 to 160 km
P^*_1	$2.3 + \Delta/6.3$	Reflections, 55 to 170 km
P^*_2	$4.2 + \Delta/6.9$	First arrival beyond 160 km
P_n	$8.7 + \Delta/7.7$	Reflections, 100 to 250 km, and Mono Lake to China Lake reciprocal point

Eaton, *CDMG Bull 190*, 1966

Note that Pn only a first arrival from north at very south end of profile

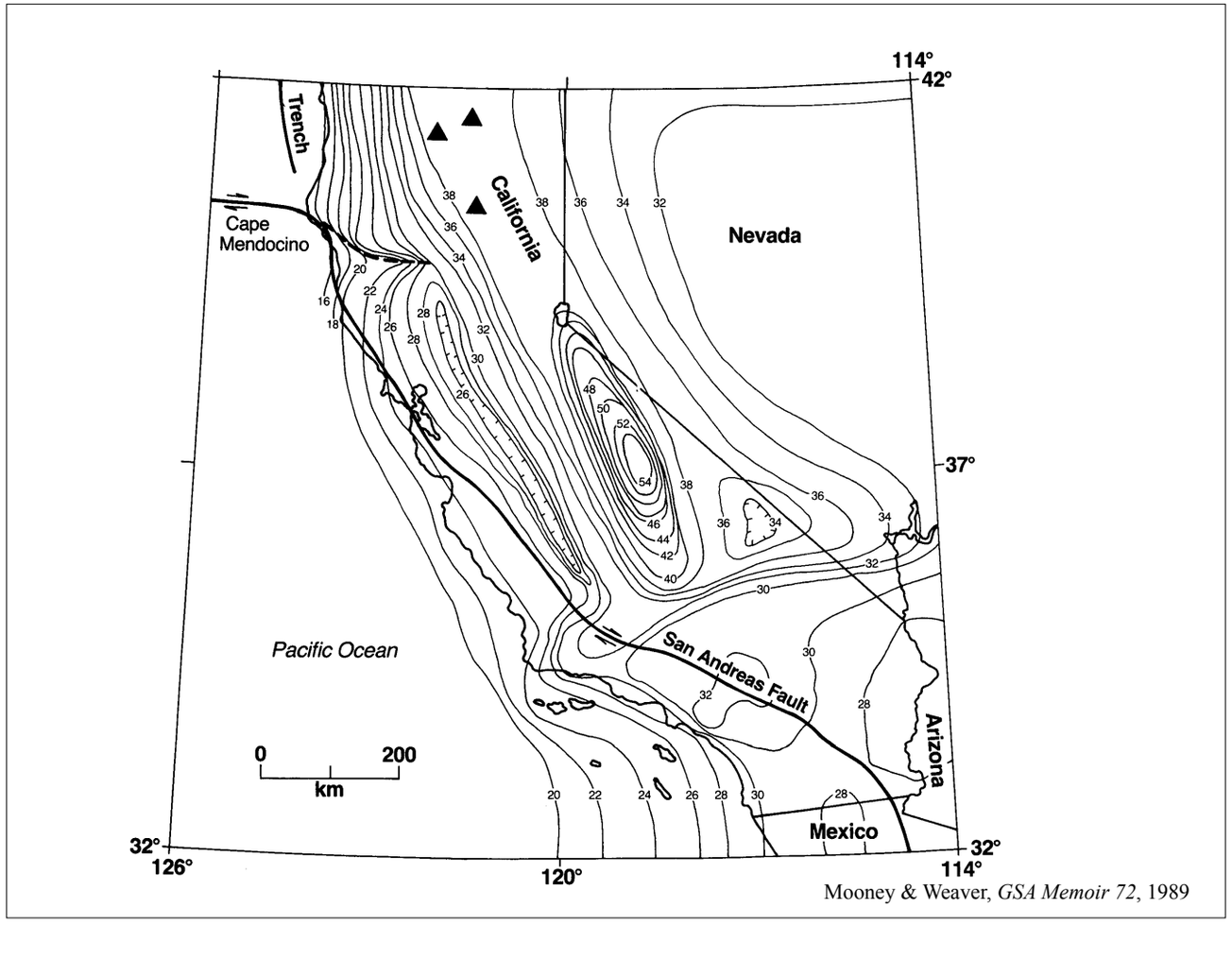

Mooney & Weaver, *GSA Memoir 72*, 1989

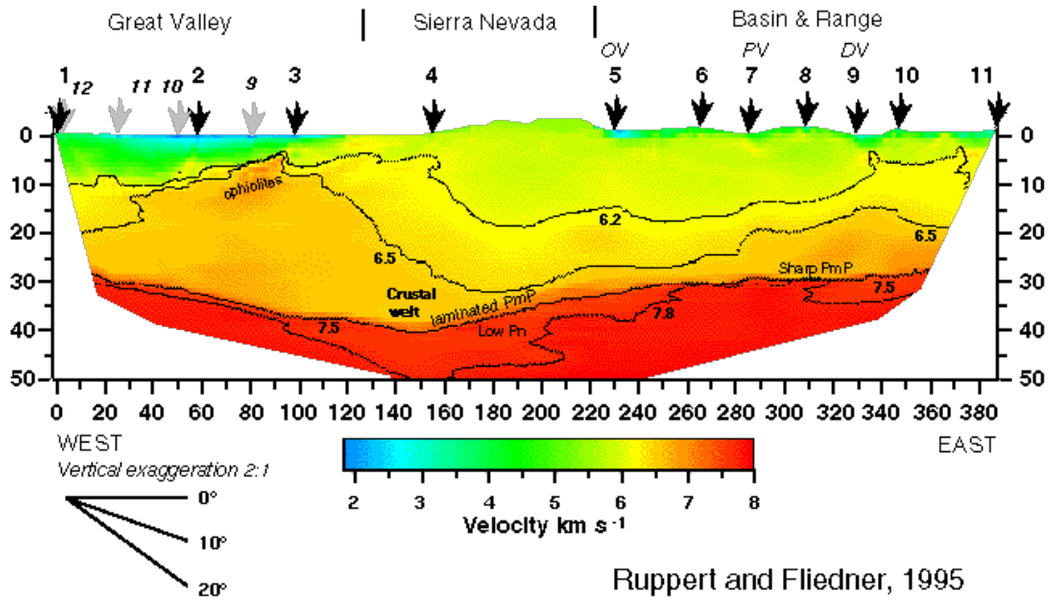

Ruppert and Fliedner, 1995

Refraction line across the southern Sierra, 1993, clearly eliminated a thick root.

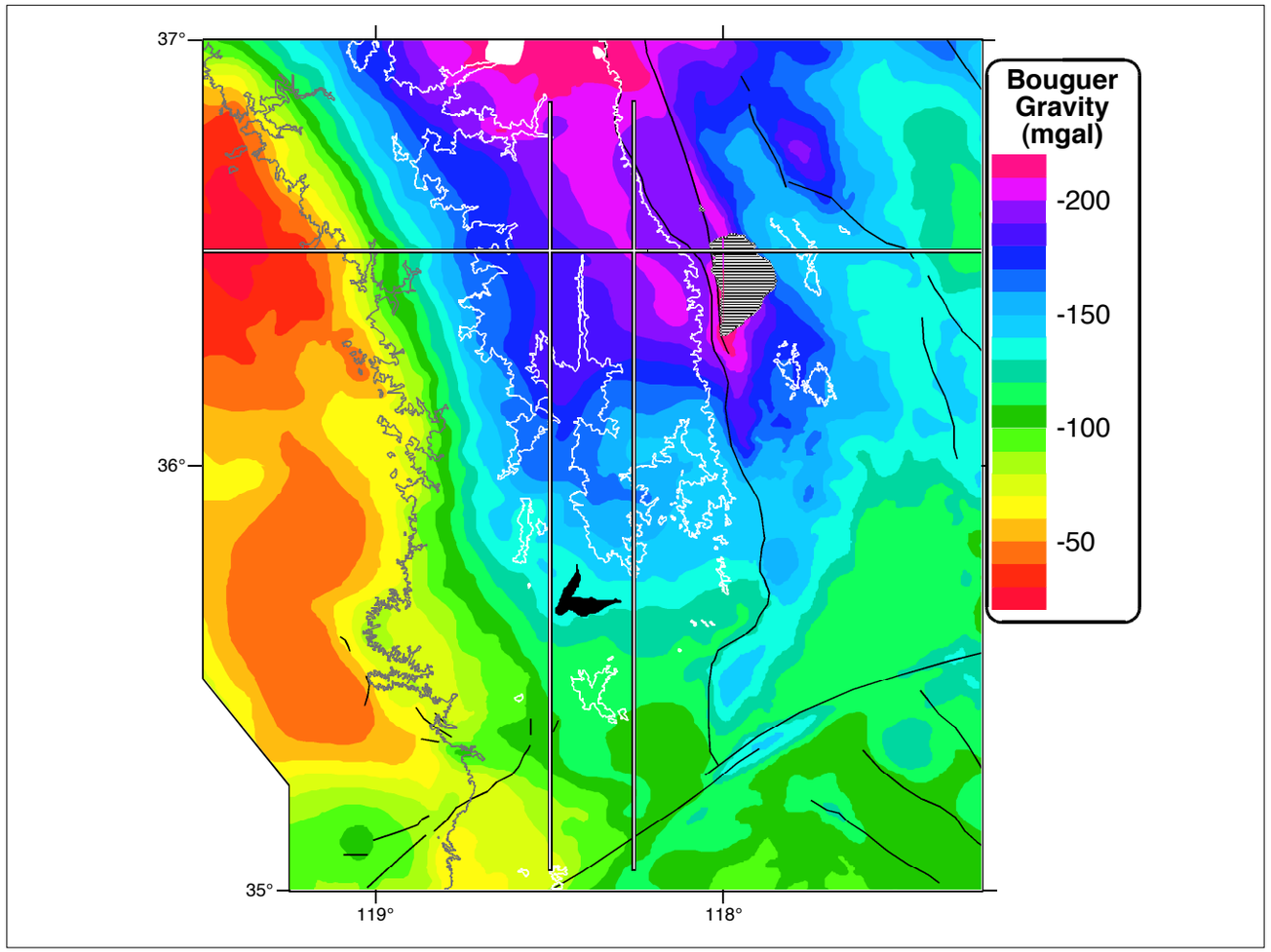
37°
36°
35°
119°
118°
Bouguer Gravity (mgal)
-200
-150
-100
-50

Airy Root

$$d = \frac{\rho_c \, \Delta h}{(\rho_m - \rho_c)}$$

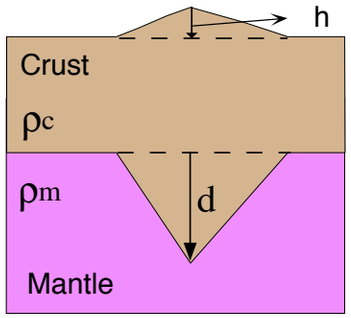

- Constant Pn velocity
- Large dips on Moho

Pratt "Crustal" Root

$$\Delta\rho = \frac{-\rho_c \, \Delta h}{(h_c + \Delta h)}$$

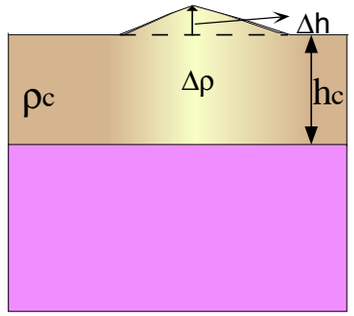

- Constant Pn velocity
- ***No*** dips on Moho
- Variations in surface geology ?

Pratt "Mantle" Root

$$\Delta\rho = \frac{-\rho_c \, \Delta h}{h_m}$$

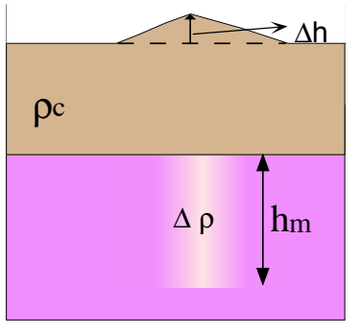

- Varying Pn velocity
- ***No*** dips on Moho
- No variations in surface geology

Jones et al., *JGR*, 1994

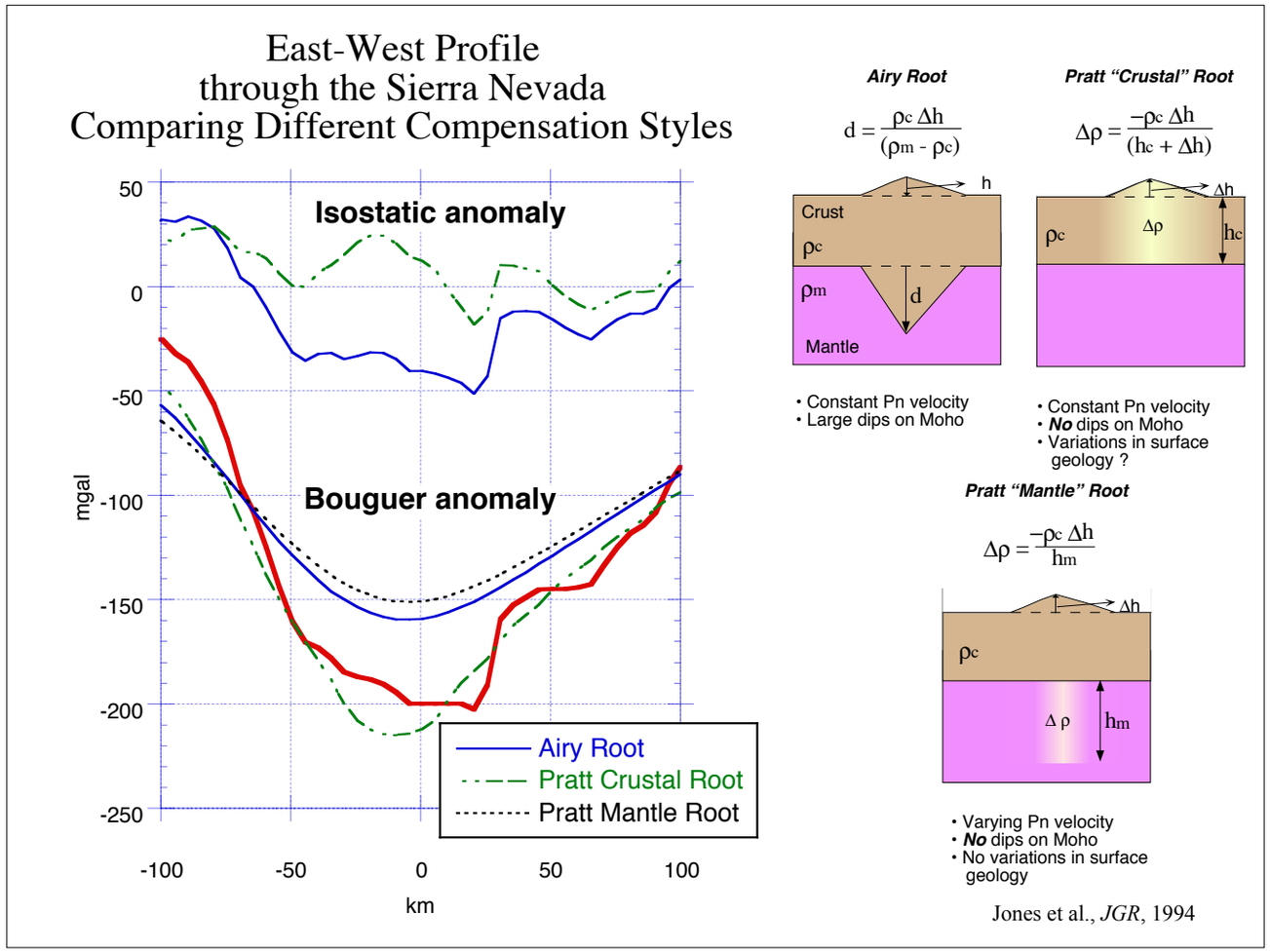

Note the large isostatic anomaly (blue line) for an Airy root but much smaller anomaly if using lateral variations in the crust

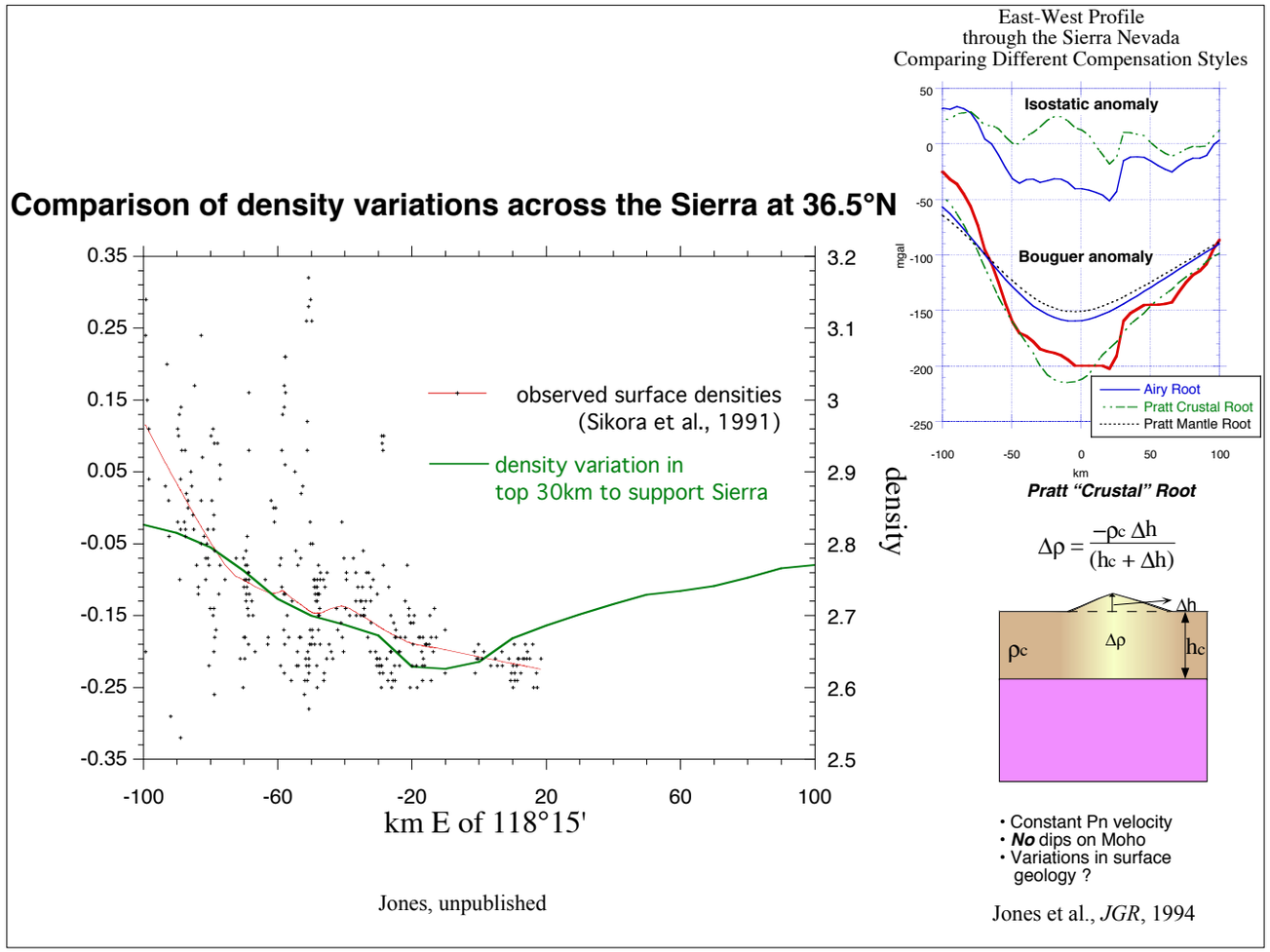

Red line is a smoothed fit to observed densities.

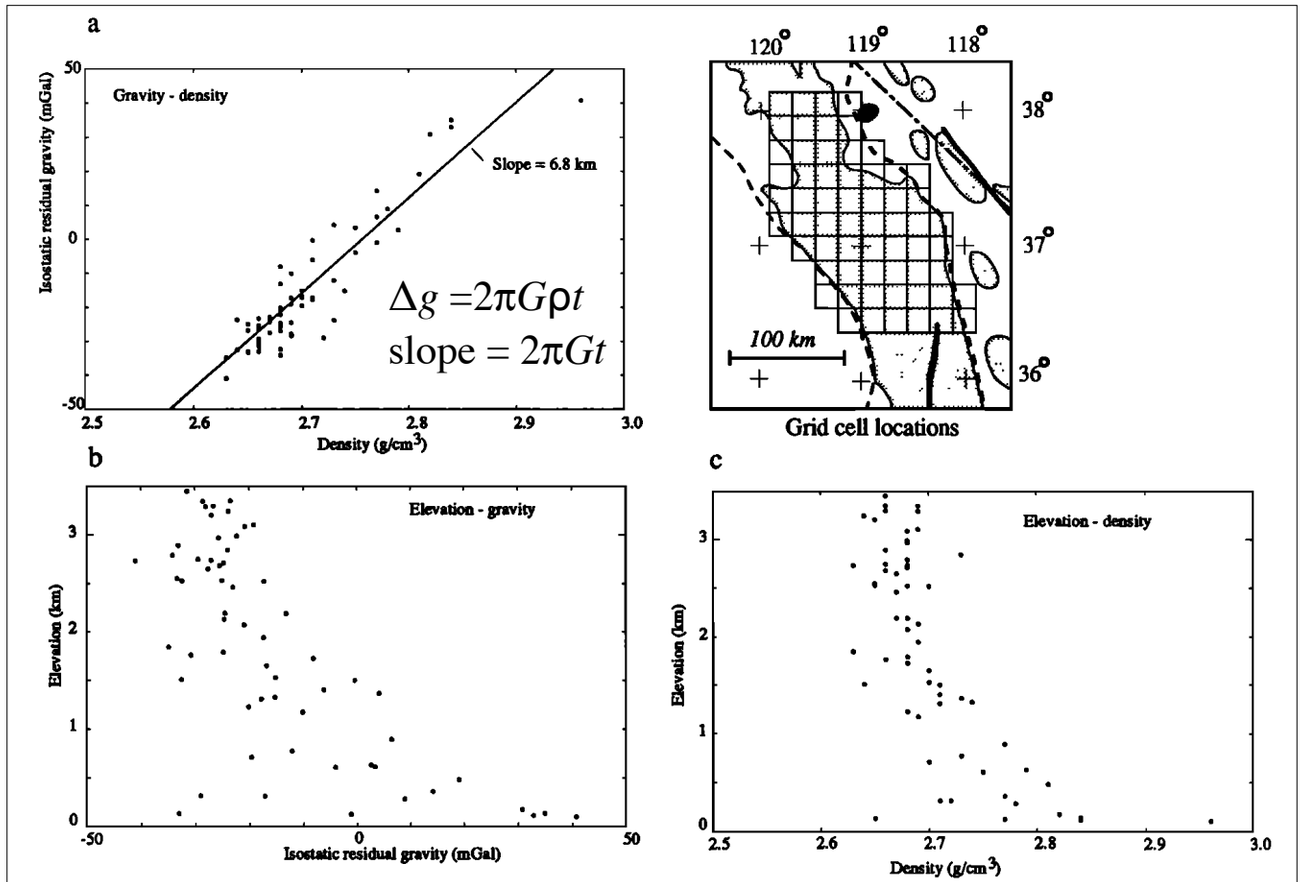

Saltus & Lachenbruch, *Tectonics*, 1991

rhoc is x, delta g is y, so slope is

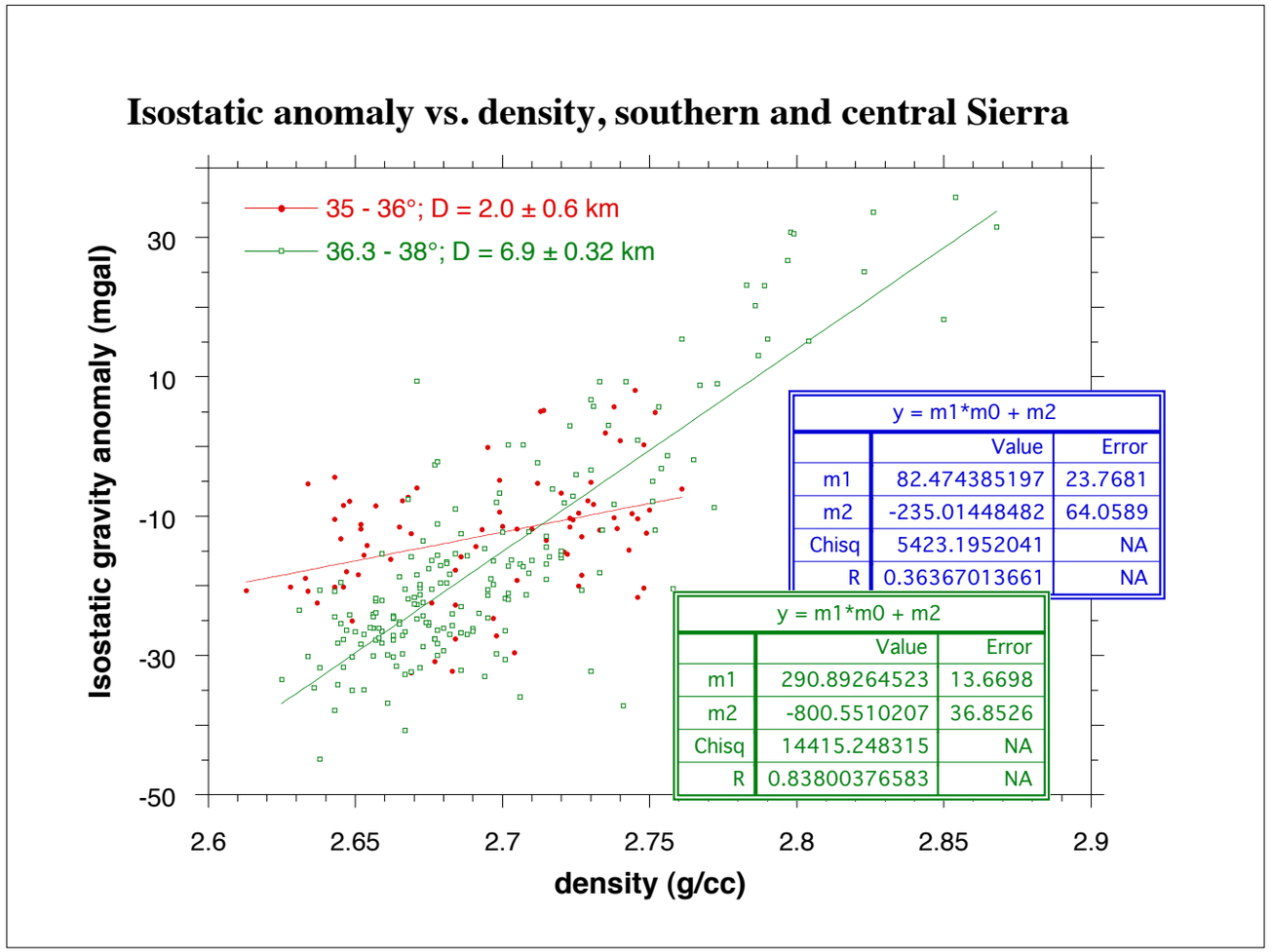
Isostatic anomaly vs. density, southern and central Sierra
35 - 36°; D = 2.0 ± 0.6 km
36.3 - 38°; D = 6.9 ± 0.32 km
Isostatic gravity anomaly (mgal)
30
10
-10
-30
-50
2.6
2.65
2.7
2.75
2.8
2.85
2.9
density (g/cc)
y = m1*m0 + m2
Value
Error
m1
82.474385197
23.7681
m2
-235.01448482
64.0589
Chisq
5423.1952041
NA
R
0.36367013661
NA
y = m1*m0 + m2
Value
Error
m1
290.89264523
13.6698
m2
-800.5510207
36.8526
Chisq
14415.248315
NA
R
0.83800376583
NA

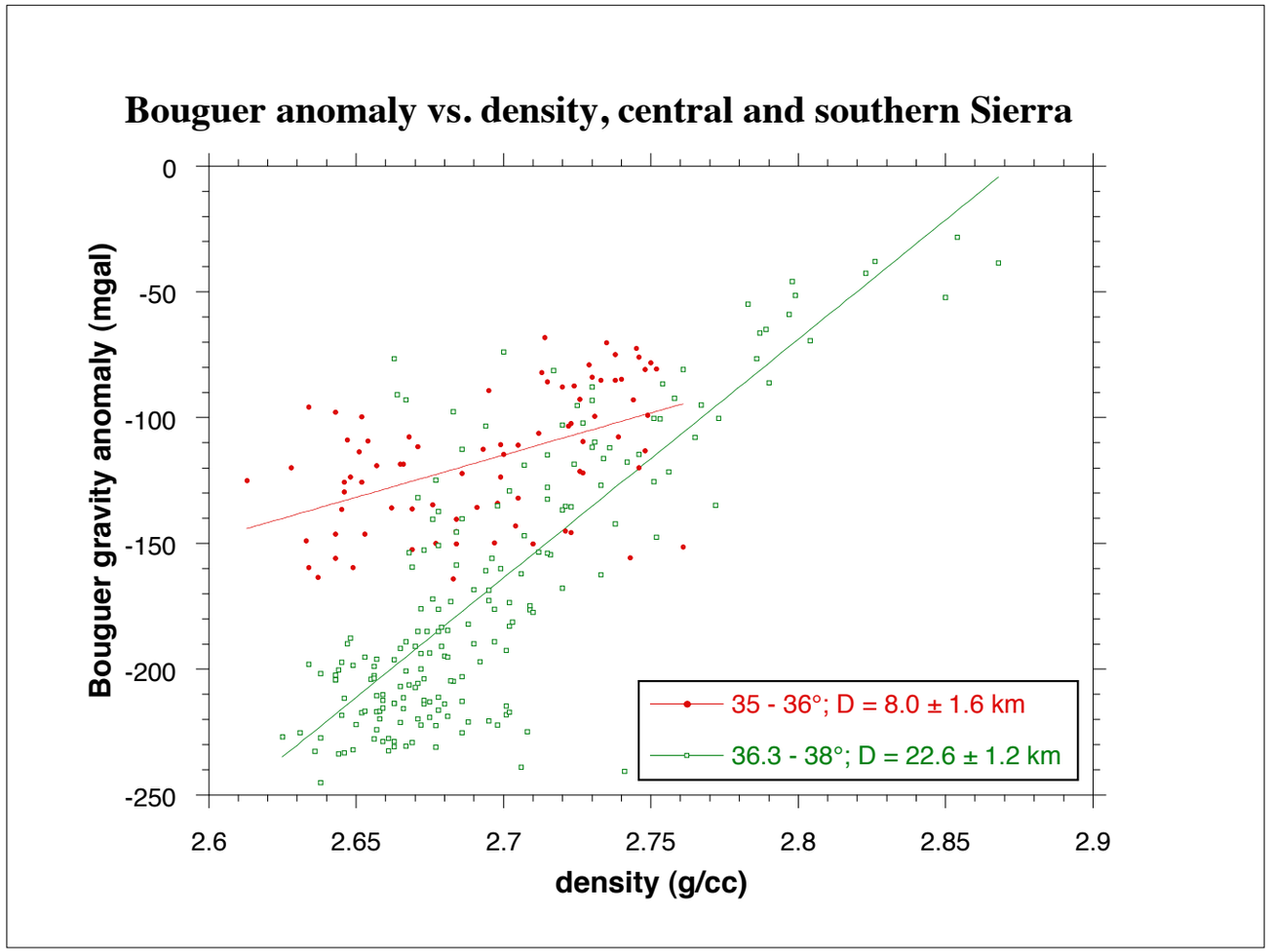
Bouguer anomaly vs. density, central and southern Sierra
Bouguer gravity anomaly (mgal)
0
-50
-100
-150
-200
-250
2.6
2.65
2.7
2.75
2.8
2.85
2.9
density (g/cc)
35 - 36°; D = 8.0 ± 1.6 km
36.3 - 38°; D = 22.6 ± 1.2 km

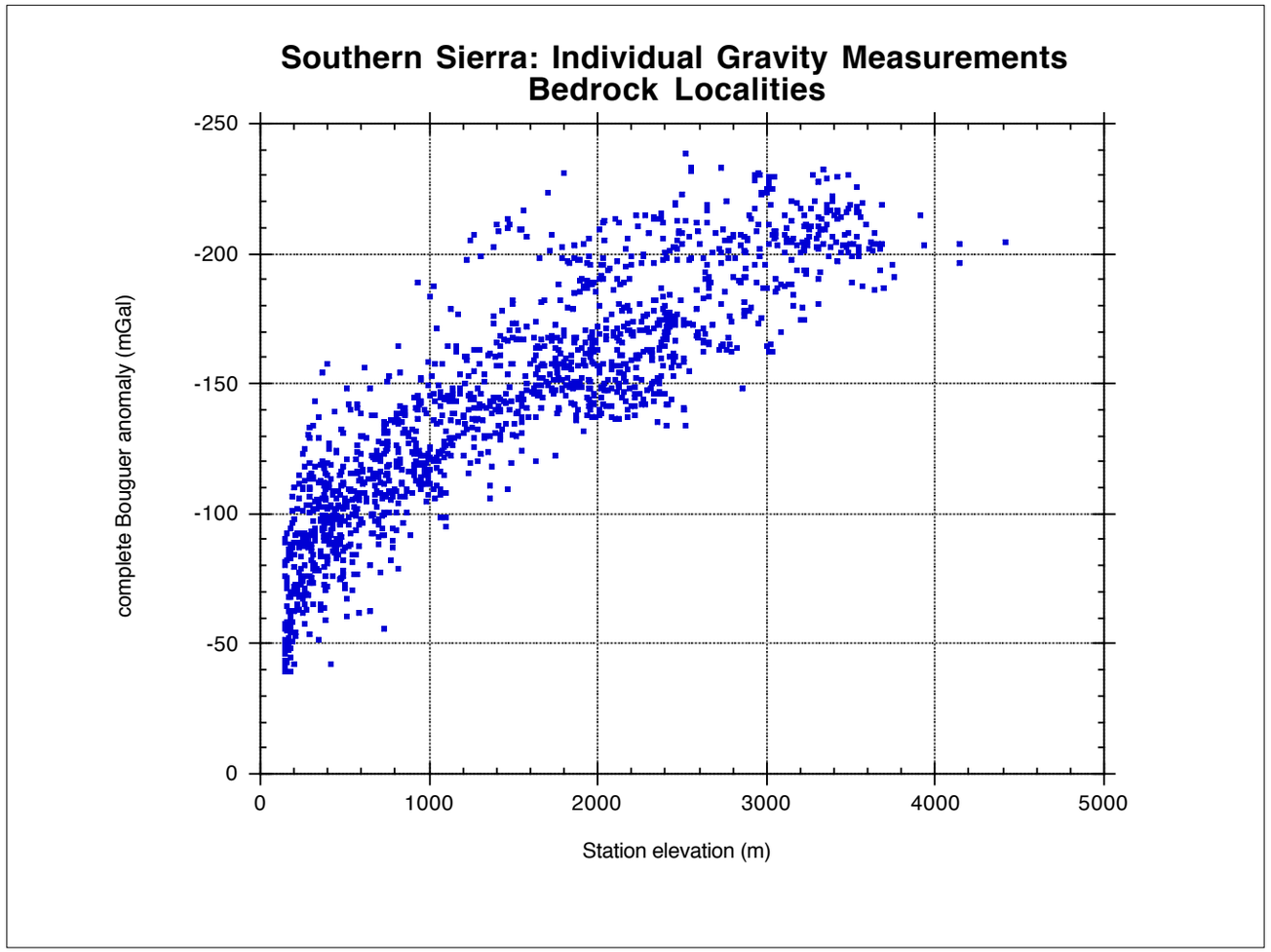
Southern Sierra: Individual Gravity Measurements
Bedrock Localities
complete Bouguer anomaly (mGal)
-250
-200
-150
-100
-50
0
0
1000
2000
3000
4000
5000
Station elevation (m)

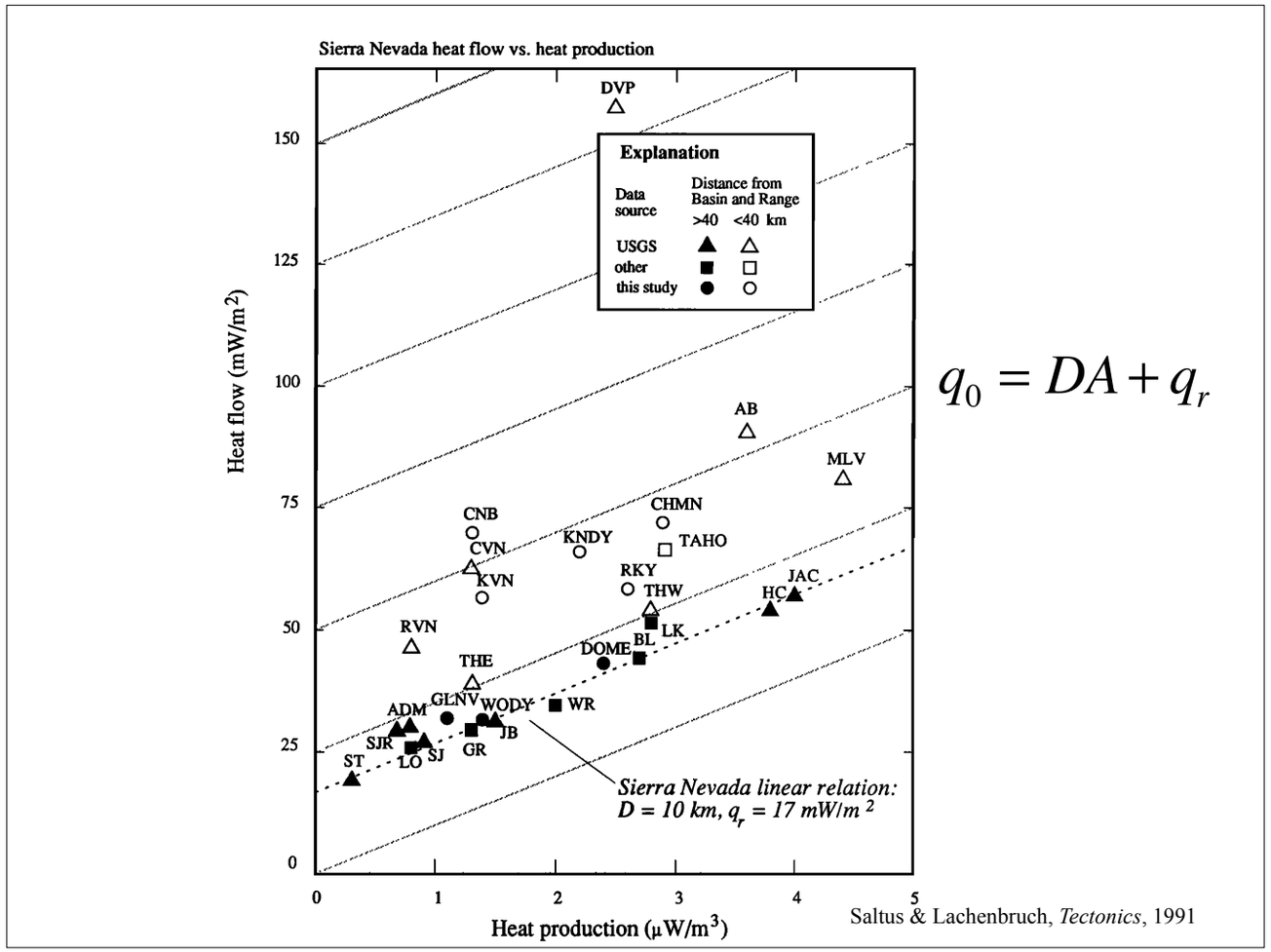

$$q_0 = DA + q_r$$

Saltus & Lachenbruch, *Tectonics*, 1991

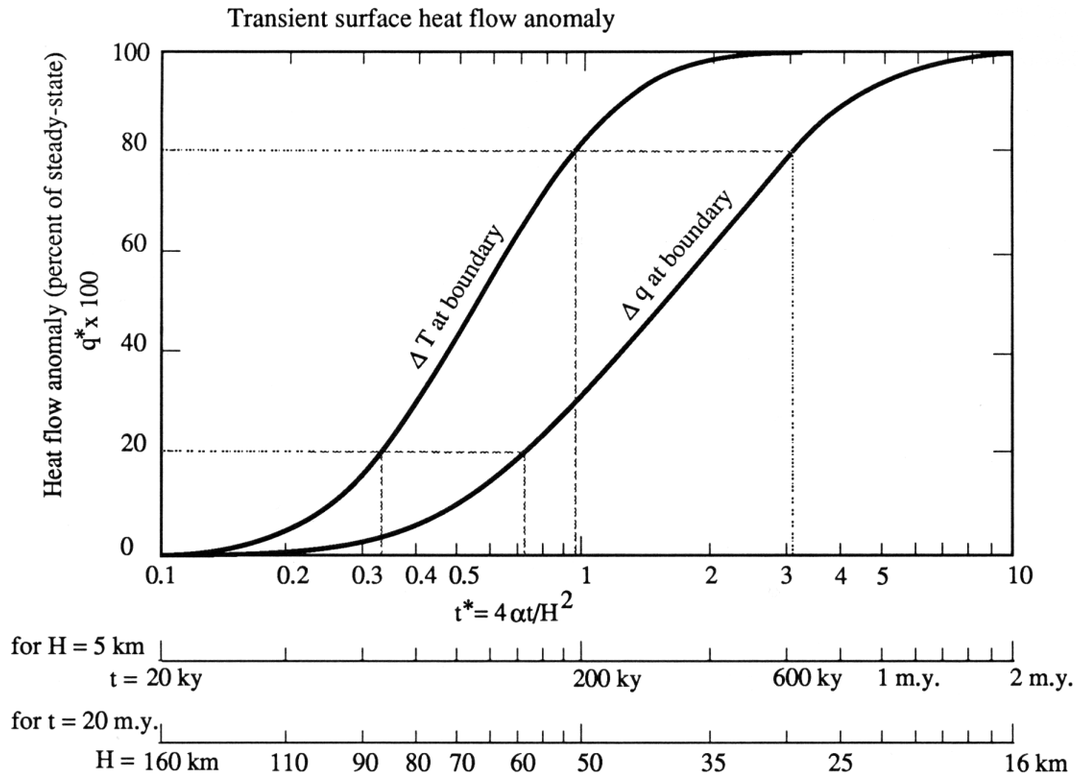

Fig. 7. Dimensionless heat flow q^* versus time t^* for the conduction of a thermal disturbance through a finite slab of thickness H. Dimensionless heat flow $q^* = q/q_\infty$ is the ratio of the transient surface heat flow q to the steady state (equilibrium) heat flow q_∞. The dimensionless time is $t^* = 4\alpha t/H^2$ where α is thermal diffusivity and t is time since the initiation of the basal thermal disturbance. Two thermal boundary conditions for the disturbance are used: ΔT is a

Saltus & Lachenbruch, *Tectonics*, 1991

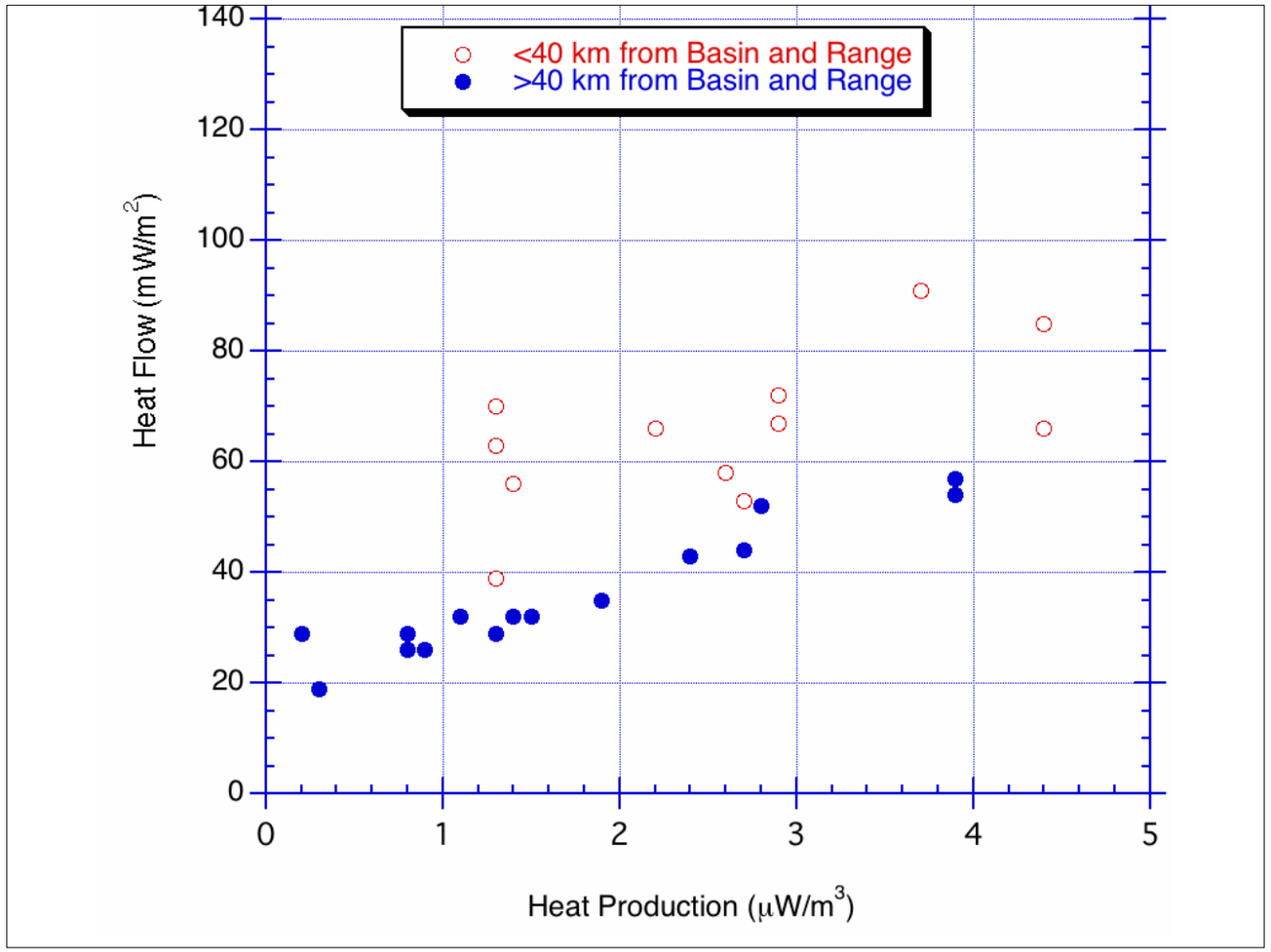
<40 km from Basin and Range
>40 km from Basin and Range
Heat Flow (mW/m^2)
Heat Production (μW/m^3)
0
20
40
60
80
100
120
140
0
1
2
3
4
5

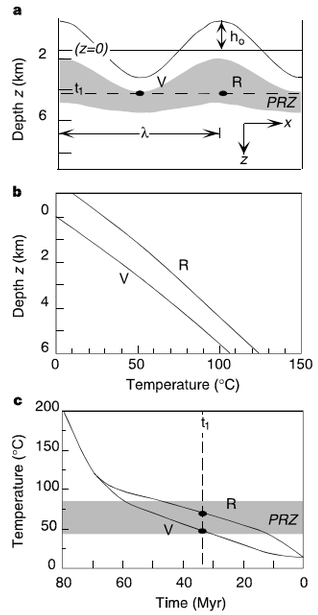

Figure 1 Thermal history of rock samples below periodic topography. **a**, Schematic range-parallel cross-section showing the influence of topography on isotherms bounding the partial retention zone (PRZ, shaded) for helium in apatite (45–85 °C; ref. 11). At time t_1 the sample below the valley (V) is nearly closed to helium diffusion, while the sample below the ridge (R) remains open, resulting in a younger (U–Th)/He age beneath the ridge. **b**, Steady-state geotherms beneath valley and ridge sites described by equation (1) using nominal central Sierran heat-flow parameters[13] of reduced heat flow q_m (21 mW m^{-1}), characteristic depth of heat production h_r (10 km), thermal conductivity k (2.4 W K^{-1} m^{-1}), surface radioactive heat production ρH_s (1 μW m^{-3}), temperature at depth $z = 0$ km T_o (15 °C), and lapse rate of mean surface temperature β (4.5 °C km^{-1}). **c**, Hypothetical cooling histories of valley and ridge samples. Rapid cooling trajectory above ~100 °C based on higher temperature thermochronometers for central Sierra[15,16]. Trajectory through PRZ assumes unroofing at a constant rate of 0.08 mm yr^{-1} of a steady-state topography with $h_o = 1$ km and $\lambda = 70$ km from a depth $z = 6$ km at 80 Myr, using geotherms from **b**.

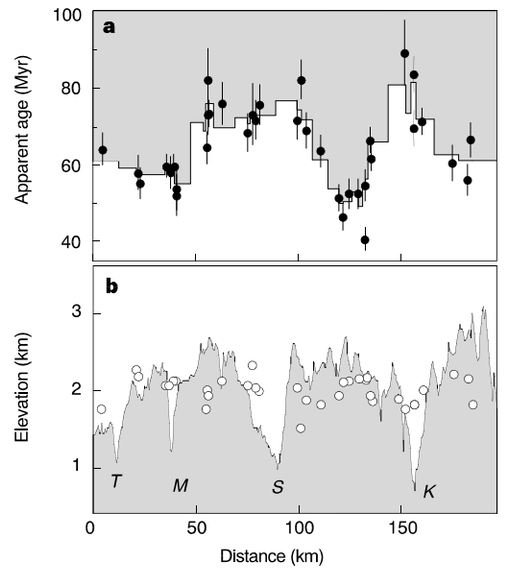

Figure 3 (U–Th)/He ages along range-parallel profile. **a**, Elevation-adjusted helium ages for samples projected onto profile in Fig. 2. Helium and U–Th analyses were performed on the same aliquots at Caltech following procedures in refs 16, 26. Samples of euhedral, inclusion-free igneous apatite from undeformed granitic plutons were analysed in replicate, with mean ages ranging from 44.5 to 84.6 Myr. Errors shown are 1σ and reflect analytical uncertainties in helium and U–Th measurements[16,26]. Ages were corrected for small differences in sample elevation above or below 2,000 m using the observed age–elevation gradient[16]. Stepped curve is defined by three-sample average of elevation-adjusted ages. A complete table of analytical results is available; see Supplementary Information. **b**, Location and elevation of samples projected onto profile in Fig. 2, plotted with topography along profile. Drainages are labelled as in Fig. 2.

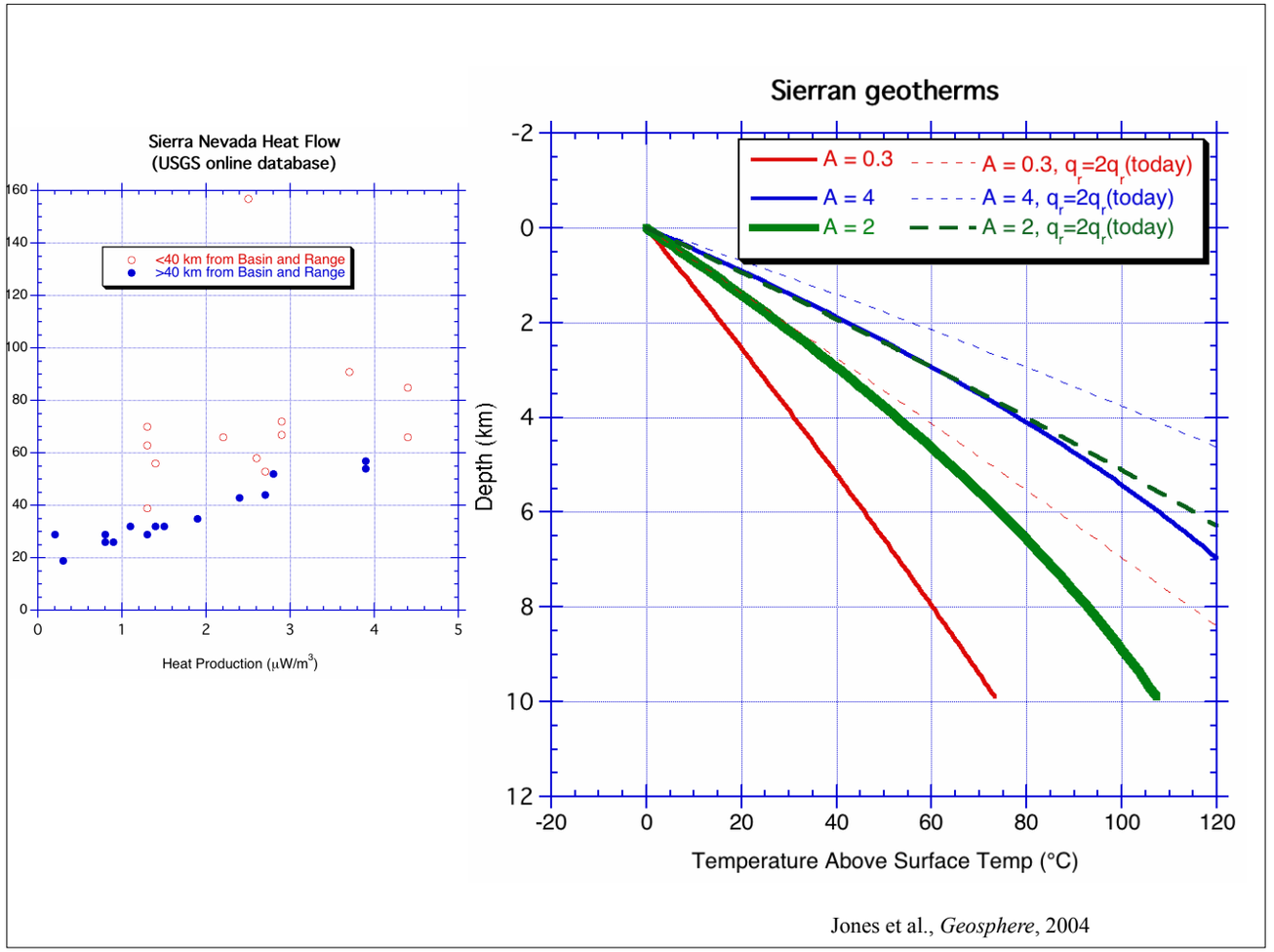

Jones et al., *Geosphere*, 2004

We know there is a big variation in heat production (left)--what is the impact on shallow geotherms

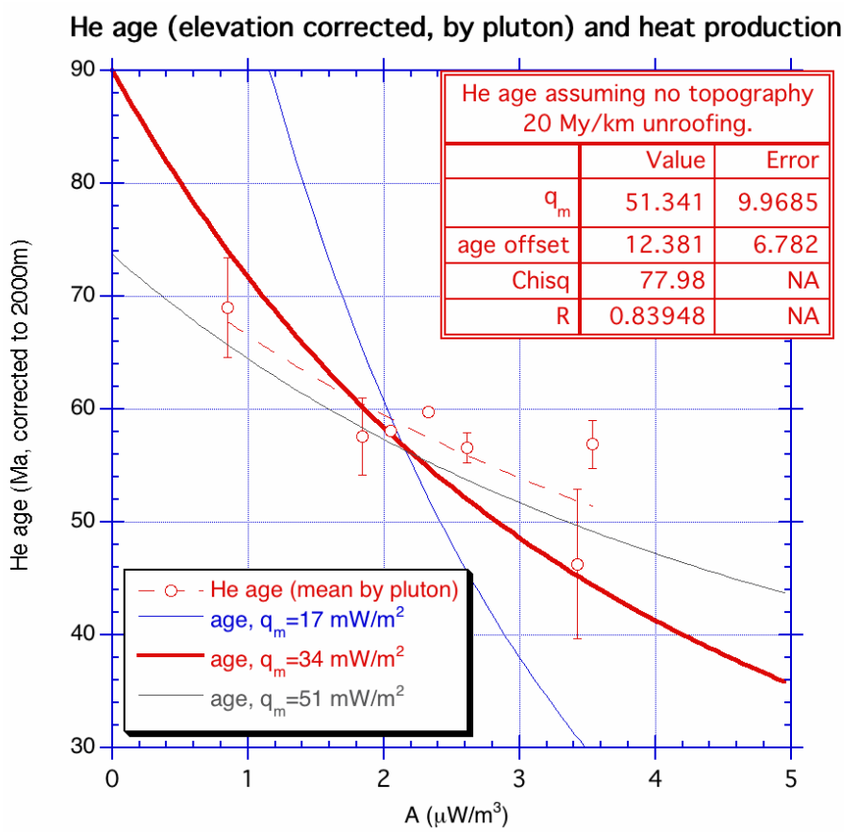

Jones et al., *Geosphere*, 2004

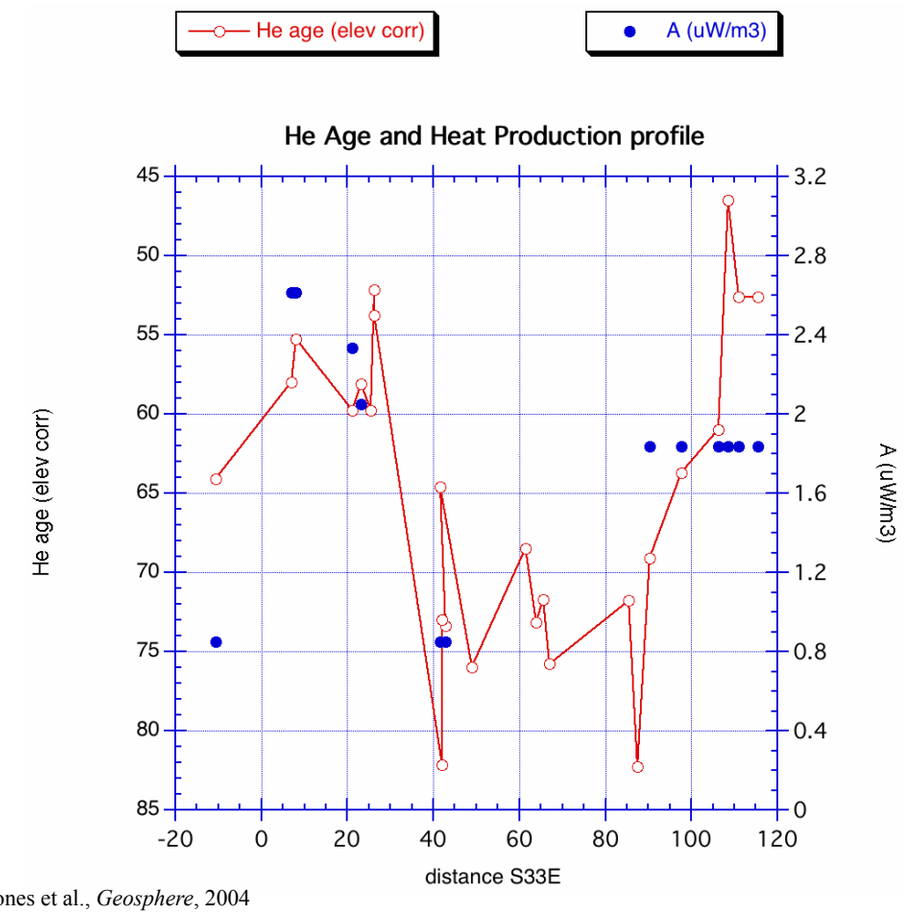

Jones et al., *Geosphere*, 2004